

ELM benchmark of the 2DX code

D. A. Baver and J. R. Myra

Lodestar Research Corporation, Boulder Colorado 80301

Maxim Umansky

Lawrence Livermore National Laboratory

1 Introduction

This test was devised to verify the ability of the 2DX eigenvalue code to solve a simple fluid model relevant to the stability threshold of edge localized modes in tokamaks. Since the functionality of the 2DX code depends on both the source code itself and the input file defining the system of equations to solve (structure file), this test demonstrates both. Moreover, since the structure file used for this test represents a subset of a more general 6-field model, many of the terms in that test are also verified.

This test compares 2DX results to BOUT++ simulations. Previous comparisons with BOUT++ are referenced for purposes of interpreting the results.

2 Description

2.1 Code structure

The 2DX code is a highly flexible eigenvalue solver designed for problems relevant to edge physics in toroidal plasma devices. Its flexibility stems from the use of a specialized input file containing instructions on how to set up a particular set of equations. Because of this, the 2DX code permits model equations to be changed without altering its source code. The drawback to this approach is that any change to the structure file represents a potential source of error, necessitating re-verification. This problem is offset by the fact that the source code remains unchanged, thus testing one structure file builds confidence in the underlying code that interprets the structure file. Also, structure files can be translated into analytic form, thus allowing the user to verify that the file contains the equations intended.

The structure file contains two main parts: an elements section, which constructs the differential operators and other functions used in a particular set of equations, and a formula section, which assembles these into an actual set

of equations. This separation means that elements can be recycled in other structure files. By testing one structure file, one builds confidence in the elements used in that file. The main source of error when switching to a different structure file then is in the formula section, which can be manually verified by translating into analytic form.

Regardless of the content of the structure file, the 2DX code is fundamentally a finite-difference eigenvalue solver. As such, it is subject to the limitations of any code of its type.

2.2 Model equations

For this test we use the following model equations [1]:

$$\gamma \nabla_{\perp}^2 \delta\phi = \frac{2B}{n} C_r n \delta T_i - \frac{B^2}{n} \partial \nabla_{\perp}^2 \delta A + i \frac{B k_b}{n} \delta A \partial_r \frac{J_{\parallel}}{B} \quad (1)$$

$$\gamma \delta T_i = -i \frac{k_b}{B} \delta\phi \partial_r T_i \quad (2)$$

$$\gamma \left(\frac{n}{\delta_{er}^2} \right) \delta A = -n \mu \nabla_{\parallel} \delta\phi \quad (3)$$

where

$$C_r = \mathbf{b} \times \kappa \cdot \nabla = -\kappa_g R B_p \partial_x + i(\kappa_n k_b - \kappa_g k_{\psi}) \quad (4)$$

$$\nabla_{\perp}^2 = -k_b^2 - jB(k_{\psi} - i\partial_x R B_p)(1/jB)(k_{\psi} - iR B_p \partial_x) \quad (5)$$

$$\partial_{\parallel} Q = B \nabla_{\parallel} (Q/B) \quad (6)$$

$$\nabla_{\parallel} = j \partial_y \quad (7)$$

In this notation, κ_g is geodesic curvature, κ_n is normal curvature, k_b is binormal wavenumber, k_{ψ} is radial wavenumber. $R B_p$ is poloidal flux density, as poloidal flux is used as a radial coordinate, j is the inverse Jacobian $1/JB$ which is used to define the poloidal coordinate, and Q is any quantity. The above equations are normalized to Bohm units, i.e. all distances are in units of ρ_s and all time scales are in units of ω_{ci}^{-1} .

2.3 Boundary conditions

This test case uses phase-shift periodic boundary conditions in the parallel direction, and zero-derivative boundary conditions in the radial direction. The phase shift in the parallel direction is given by:

$$\delta Q(y=0) = \delta Q(y=2\pi) e^{-i2\pi nq} \quad (8)$$

This ensures toroidal and poloidal periodicity in the field-line following coordinate.

2.4 Profile setup

The formulas in Eq. 1-3 are normalized to Bohm units. Values are converted by dividing input distances by ρ_s , and input magnetic fields are in Tesla. Output eigenvalues are multiplied by ω_{ci} .

The geometry used is a thick annulus. This annulus contains a self-consistent equilibrium magnetic field, current profile, and pressure profile. This profile is based on a specific data file [2], further details of which are provided later in this document in Figs. 2-4.

3 Numerical results

The code was tested by sweeping toroidal mode number from 5 to 100 and comparing with BOUT++ results. Growth rates were normalized by dividing by ω_A . This is calculated from the reference values $B=1.9412991$ T, $R=3.49717$ m, and $n=1.01 \times 10^{20}m^{-3}$, yielding a value $\omega_A = 8.51707 \times 10^5$. The results of this test are shown in figure 1. In addition, the raw data is shown in table 1.

These results show good agreement between the two codes for low toroidal mode numbers. Significant disagreement occurs at higher mode numbers. However, the amount of disagreement decreases rapidly with higher radial resolution in the BOUT++ simulations. Moreover, a similar discrepancy pattern was noted in a previous comparison of BOUT++ to ELITE [1].

3.1 Convergence study

In order to estimate the accuracy of the previous results, and in order to estimate error scaling with resolution, a convergence study was done. In this study, the $n = 50$ mode was calculated on grids with varying resolution in n_x and n_y . Each of these parameters was varied in multiples of two, with n_x ranging from 64 to 1024, and n_y ranging from 16 to 64. For each value of n_y , Richardson extrapolation was performed in n_x in order to estimate a correct value and to calculate a power law for error scaling. The corrected values were then used to perform Richardson extrapolation a second time in n_y .

The results of this study are shown in Figs. 5-6. The n_x scan for $n_y=64$ yielded a power law of $\epsilon \propto n_x^{-2.64323}$ with other n_y values giving similar power laws. The n_y scan of the extrapolated values yielded a power law of $\epsilon \propto n_y^{-1.94741}$. The final extrapolated value (normalized to ω_A) is .363751.

References

- [1] B. D. Dudson *et al*, Comp. Phys. Comm. **180** (2009) 1467.

- [2] P. Snyder, data file cbm18-dens8-y064-x260.grd.pdb.v2.hdf

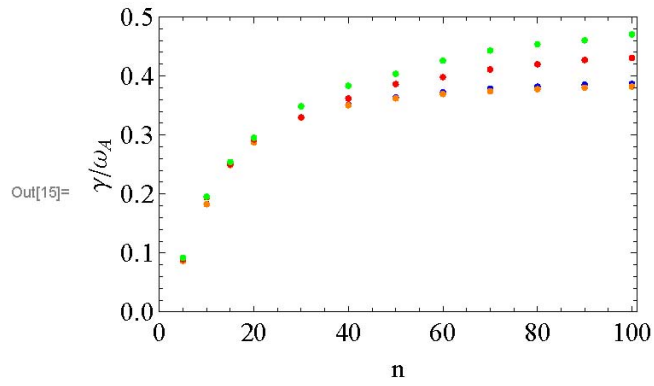


Figure 1: Growth rate vs. toroidal mode number for ELM models on 2DX and BOUT++. The blue dots are 2DX results for $n_x=512$, the orange dots are 2DX results for $n_x=256$, the red dots are BOUT++ results for $n_x=512$, and the green dots are BOUT++ results for $n_x=256$.

| n | $Re(\gamma)/\omega_A$ 2DX (nx=512) | $Re(\gamma)/\omega_A$ 2DX (nx=256) | γ/ω_A BOUT++ (nx=512) | γ/ω_A BOUT++ (nx=256) |
|-----|------------------------------------|------------------------------------|-----------------------------------|-----------------------------------|
| 5 | .0865383 | .0864301 | .0894333 | .0916790 |
| 10 | .182753 | .182911 | .194466 | .195453 |
| 15 | .248903 | .249047 | .250183 | .254074 |
| 20 | .287606 | .287774 | .292470 | .295150 |
| 30 | .329408 | .329749 | .330025 | .348405 |
| 40 | .350433 | .351111 | .361835 | .383246 |
| 50 | .362255 | .363654 | .386312 | .403599 |
| 60 | .369492 | .372193 | .398018 | .426154 |
| 70 | .374249 | .378379 | .410997 | .443173 |
| 80 | .377585 | .381714 | .419887 | .453644 |
| 90 | .380091 | .385232 | .427058 | .460371 |
| 100 | .382127 | .386651 | .430449 | .470444 |

Table 1: Growth rate vs. toroidal mode number for 2DX vs. BOUT++

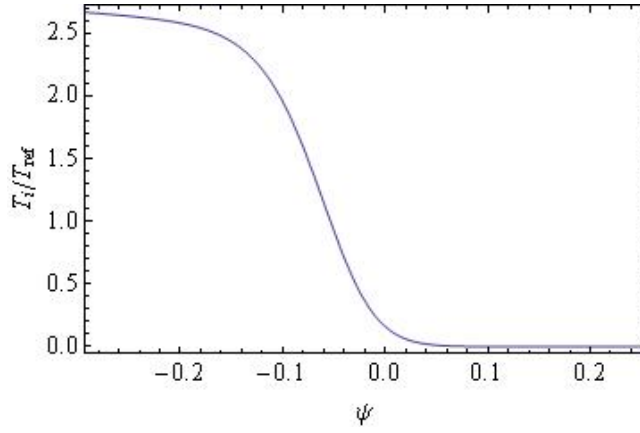


Figure 2: Ion temperature as a function of poloidal flux for the ELM profile.

Temperature is normalized to $T_{ref} = 635.2eV$. Note that these values are doubled compared to the original data file in order for the ion temperature equation to also capture the effects of electron pressure.

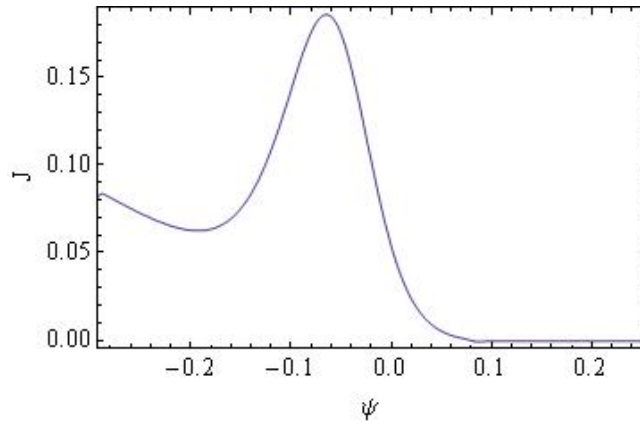


Figure 3: Current as a function of poloidal flux for the ELM profile. Current is normalized to $n_e c_s$ where $n_e = 1.01 \times 10^{14}$ and $c_s = 1.74143 \times 10^7$ in cgs units.

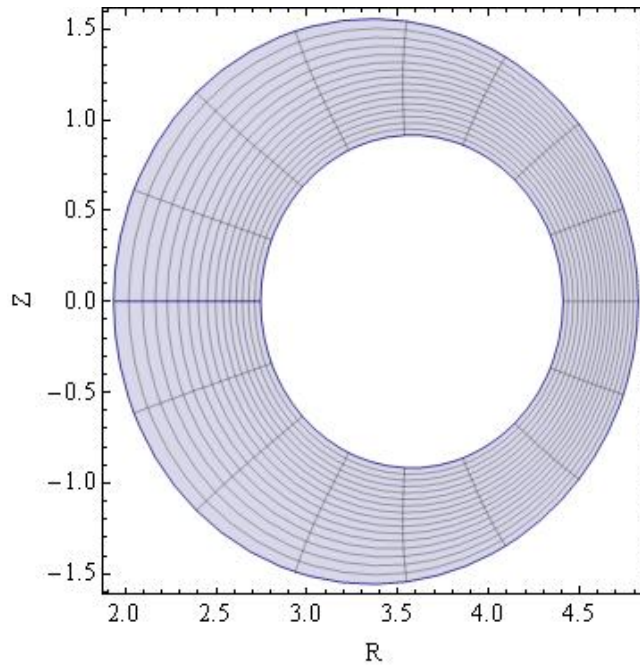


Figure 4: Flux surfaces in physical space for the ELM profile.

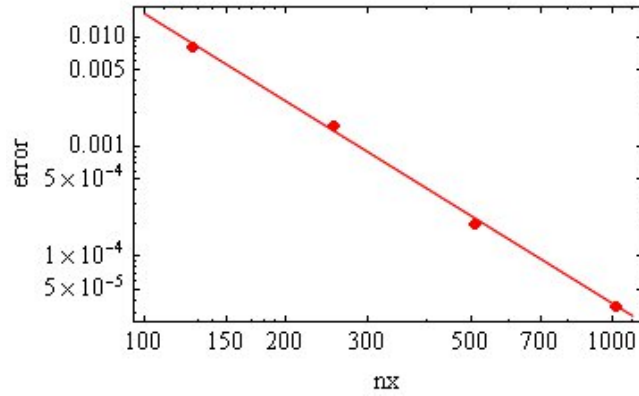


Figure 5: Convergence with increasing n_x for the ELM $n=50$ case at $n_y=64$

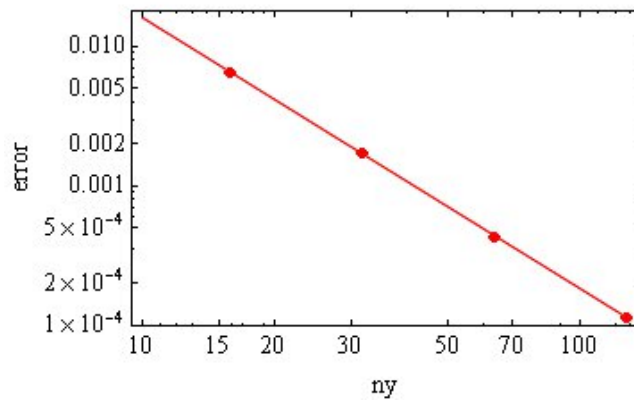


Figure 6: Convergence with increasing n_y for the ELM $n=50$ case.